Applied Catalysis B: Environmental 127 (2012) 389–398

Contents lists available at SciVerse ScienceDirect

Applied Catalysis B: Environmental

journal homepage: www.elsevier.com/locate/apcatb

CO_x free hydrogen production over cobalt incorporated silicate structured mesoporous catalysts

Dilek Varisli*, Nalan G. Kaykac

Advanced Technologies, Gazi University, 06500, Ankara, Turkey

ARTICLE INFO

Article history:
Received 16 April 2012
Received in revised form 3 August 2012
Accepted 30 August 2012
Available online 8 September 2012

Keywords:
Hydrogen
Ammonia decomposition
Cobalt
Catalyst
Mesoporous silicate
Hydrothermal synthesis

ABSTRACT

On board hydrogen production for fuel-cell derived motor vehicles requires resources for CO_x free hydrogen production. Ammonia is one of the most attractive hydrogen storage compounds which may yield clean hydrogen through catalytic decomposition. In the present study, new cobalt incorporated mesoporous silicate catalysts were prepared for ammonia decomposition, by applying a one-pot hydrothermal synthesis procedure. Ammonia decomposition experiments were performed in a fixed bed flow reactor in a temperature range of 400–750 °C. While all of the synthesized catalysts showed good activity in hydrogen production from ammonia at temperatures higher than 500 °C and at a space velocity of 150,000 h^{-1}, catalysts prepared with KOH promoter gave the highest activity with 70% conversion at 600 °C and close to total conversion at 700 °C. Reduction temperature and period of the synthesized catalysts were also shown to be highly effective on the catalytic performance of the synthesized materials.

1. Introduction

Hydrogen is considered to be one of the most important clean energy sources and it can be utilized by means of fuel cells. Due to the limitations in storage and delivery of hydrogen, its on-site generation has attracted the attention of researchers [1]. For the on-board production of hydrogen, reforming of alcohols (methanol or ethanol) was proposed in some of the recent studies [2]. However, formation of CO_x byproducts, especially CO, resulted in a decrease in cell performance even at extremely small concentrations [3–5]. More recently, ammonia (NH_3) has been considered as an important alternative feedstock to produce CO_x free hydrogen [1]. It has high energy density (3000 Wh/kg) and higher hydrogen storage capacity (17.7 wt%) in comparison to methanol. Consequently it is considered to be one of the best alternates for hydrogen storage in fuel cell derived transportation vehicles [6]. Moreover, it is clean, its storage or transportation is not a problem since it is in liquid form at room temperature under the pressure of 10 bar [7]. In addition, the only side product is nitrogen in the case of its decomposition [5,8].

Different metals, such as Pt [9], Ru [4,8,10–15], Rh [9], Fe [5,7,16–20], Pd [9], W [21], Ni [1,4,10,22,23], Ir [10] have been tested in ammonia decomposition reaction. Utilization of different supports such as Al_2O_3 [1,10,23], ordinary silica SiO_2 [10], carbon [7,24], carbon nanotubes [11], zeolite [13] was also mentioned for the synthesis of metal impregnated catalysts for ammonia decomposition reaction. Carbon based supports, such as carbon nanotubes, have been frequently used due to their good electron conductivity properties. However, undesired methanation reaction may take place at high temperature in the presence of hydrogen [4,8].

MCM-41 and SBA-15 like mesoporous silicate structured materials have high surface area with well-ordered pore structures and high thermal stability. Due to their larger pore sizes than zeolites, these mesoporous materials also create much less diffusional resistances in catalytic reactions. These properties make these materials attractive catalyst supports. There are very few studies published in the literature for ammonia synthesis over such mesoporous catalytic materials. In study of Li et al. [4] it was indicated that Ni and Ru supported mesoporous silicate materials, especially MCM-41, were very active in ammonia decomposition reaction. In another study, the feasibility of silica-coated Fe nanoparticles compared to the naked Fe nanoparticles was investigated and the iron nanoparticles encapsulated by microporous and mesoporous silica shells were found to be highly stable and active [5].

In the literature, alkali or alkaline earth metal ions were reported as efficient promoters for supported Ru and Fe catalysts for ammonia decomposition reaction [3,4,8,17]. They were found to be good at preventing sintering of Ru or Fe [4] and in some cases their usage resulted in the modification on the basicity of the support, which was in turn resulted in an enhancement of the catalytic activity of the catalyst [3]. Li et al. [4] indicated that the effect of potassium as

* Corresponding author. Tel.: +90 312 2023701; fax: +90 312 2023710.
E-mail address: dilekvarisli@gazi.edu.tr (D. Varisli).

0926-3373/$ – see front matter © 2012 Elsevier B.V. All rights reserved.
http://dx.doi.org/10.1016/j.apcatb.2012.08.042

a promoter highly dependent on the metal as well as the support used in the synthesis of the catalyst.

Cobalt-silicate catalysts were studied by different researchers [25–40] for different reactions and in these studies catalysts were mostly prepared by impregnation procedures. These catalysts were generally utilized as Fischer–Tropsch catalysts. Their application to ammonia decomposition reaction is very rare. Lendzion-Bielun et al. [41] investigated catalytic decomposition of ammonia over cobalt oxide catalysts and they reported that Co was more effective than the iron catalyst while in ammonia synthesis reaction cobalt supported catalyst seemed to be less active than the iron catalysts.

The main objectives of the present study are the synthesis of Co incorporated silicate structured mesoporous materials, by following a one-pot hydrothermal procedure and testing of catalytic performances of these materials in CO_x free hydrogen production by ammonia decomposition. These catalysts were synthesized with different Co/Si ratios in the synthesis solution using different silicate sources. Different reduction temperatures and the addition of KOH as a promoter were also tested. Activity comparison of the synthesized materials was made at different temperatures and space velocities in a fixed bed flow reactor.

2. Experimental

Cobalt based mesoporous silicate catalysts were prepared by using a one-pot hydrothermal synthesis procedure. The procedure used in this work is a modified version of the procedure used in our recent work for the synthesis of heteropolyacid incorporated mesoporous materials [42]. According to this procedure, cethyltrimethyl ammonium bromide (Merck) was used as the surfactant and 87 ml of deionized water was used to solve 13.2 g of surfactant. After a clear solution was obtained, a silicate source was added dropwise. While applying this procedure, two different silicate sources, namely, sodium silicate (Merck) and tetraethylorthosilicate, TEOS (Merck), were used. The pH of the final synthesis solution was either basic or acidic according to the used silicate source. In this study, cobalt nitrate (Matheson Coleman & Bell) was selected as the cobalt precursor and it was used in an amount to adjust the molar ratio of Co/Si in the synthesis solution at 0.05–0.15. When sodium silicate was used, the pH of the synthesis solution was around 11.9 and it was decreased to 11 by using 4 N H_2SO_4 solution before the addition of cobalt precursor. When TEOS was used as the silicate source, the pH of the synthesis solution was around 3.8 and the synthesized catalysts were called as CS1, CS2 and CS3. The catalysts prepared with sodium silicate were called as CS4, CS5 and CS6. In order to understand the effects of a basic promoter, a new set of catalysts namely CS7, CS8 and CS9 was also prepared using KOH as a promoter. TEOS was used as the silicate source in the synthesis of KOH promoted materials, adjusting the Co/Si molar ratio in the range of 0.05–0.15. When the addition of TEOS was completed, a dropwise addition of KOH was started. This process was continued until the pH of the synthesis solution reached to 11 and then cobalt nitrate solution was added. The amount of KOH used in the preparation of the synthesis solution for each of the catalyst was presented in Table 1. For all the synthesized catalysts, the final synthesis solution was put in a Teflon lined autoclave for hydrothermal synthesis at 120 °C for 96 h. The obtained product was washed with deionized water until the pH of the residual water became constant. After drying at 40 °C under vacuum condition, the final product was calcined at 550 °C under the flow of dry air.

Synthesized catalysts were characterized by different techniques. Surface area and pore size distribution of the catalysts were determined by the nitrogen adsorption–desorption analyses which were carried out by Quantachrome Autosorb-1-C/MS instrument after the samples were degassed at 110 °C for 16 h. X-ray diffraction analyses were performed by a Rigaku D/MAX2200 diffractometer with a Cu Kα radiation source with a 2θ scanning range between 1° and 90°. The crystallite size of Co_3O_4 was calculated using Scherrer's equation considering the 2θ value of diffraction line (3 1 1) peak. In order to get information about bulk composition and SEM photographs, SEM-EDX analyses were done by JSM-6400 (JEOL) equipped with NORAN system six. TGA–DTA analysis was carried out to determine the appropriate temperature for calcination using Dupont 951 Thermal Analysis equipment with a heating rate of 20 °C/min in a flow of air having a flow rate of 100 cc/min. In order to see the morphology, texture, and porosity of the synthesized catalysts, TEM analyses were carried out by JEOL JEM 2100F HRTEM with a maximum acceleration voltage of 200 kV. Before the analysis, each sample was dispersed in ethanol and one drop of this suspension was deposited on a grid covered by C-film. X-ray photoelectron spectroscopy analyses of the synthesized samples were carried out on PHI-5000 Versaprobe using Al as the X-ray anode, with an excitation power of 17.6 W.

The catalytic activity of the synthesized catalysts was tested in a fixed bed flow reactor system. A stainless steel reactor having an inner diameter of 1/4 in. was packed with 0.1 g of fresh catalyst and supported from both sides with quartz wool. This reactor was placed in a temperature controlled tubular furnace to carry out activity tests in the temperature range of 400–750 °C. Pure gaseous ammonia was fed to the system at a flow rate of 250 ml/min (Q_o), at room temperature. Some of the experiments were also repeated at a lower flow rate of ammonia, such as 60 ml/min, to see the effect of space velocity on ammonia conversion. Prior to the activity test, fresh catalyst was in situ reduced at 400 °C for 2 h under the flow of pure hydrogen (60 ml/min) in most experiments and then purged with pure argon for 30 min at the same temperature. A set of experiments was repeated over a catalyst reduced at 500 °C for 2 h to investigate the effects of reduction temperature on the catalytic performance. Another set of experiments was performed by changing the reduction time interval of the catalyst, in 60–180 min interval, keeping the reduction temperature at 400 °C. Online analysis of products was made by a Gas Chromatograph equipped with TCD and Porapak Q column. Argon was used as the carrier gas. Conversion of ammonia to hydrogen was evaluated basing on the data taken form the effluent stream.

$$X = \frac{F^0_{NH_3} - F_{NH_3}}{F^0_{NH_3}} \quad (1)$$

$$F^0_{NH_3} = F_{NH_3} + 2F_{N_2} \quad (2)$$

Each data point given in the conversion graphs was the average of at least four results obtained from successive measurements obtained at steady state. Also, overall hydrogen production rate per gram of catalyst was defined as

$$R = \frac{(F^0_{NH_3} \times X) \times (3/2)}{m_{catalyst}} \quad (3)$$

3. Results and discussion

3.1. Catalyst characterization results

In order to get a porous structure, the surfactant should be removed from the synthesized material by a calcination process. The calcination temperature was determined using thermal analysis (TGA/DTA) of the uncalcined material. TGA/DTA analysis result of an uncalcined cobalt based mesoporous silicate catalyst is presented in Fig. 1. The weight loss observed at a temperature interval of 25–115 °C was due to the removal of physisorbed water molecules. Two other weight loss ranges were observed at around 200–320 °C and at 400–500 °C. The weight loss observed between

Table 1
Physical properties of the synthesized catalysts.

Catalyst	Silicate source	Molar ratio of Co/Si in the synthesis solution	KOH used in the synthesis solution (g)	BET surface area (m^2/g)	BJH_{ads} surface area (m^2/g)	BJH_{ads} pore diameter (nm)	BJH_{ads} pore volume (cc/g)
CS1	TEOS	0.05	–	317	344	16.9	1.29
CS2	TEOS	0.10	–	228	241	29.5	1.45
CS3	TEOS	0.15	–	192	203	32.0	1.71
CS4	Sodium Silicate	0.05	–	741	839	2.2	1.11
CS5	Sodium Silicate	0.10	–	640	780	2.7	1.34
CS6	Sodium Silicate	0.15	–	335	372	3.1	1.07
CS7	TEOS	0.05	1.04	577	699	3.1	2.39
CS8	TEOS	0.10	1.30	531	611	3.0	2.42
CS9	TEOS	0.15	1.82	533	626	2.7	1.73

200 and 320 °C was explained with the decomposition and removal of organic template. Indeed, it was also indicated in the work of Varisli et al. [42] that the removal of surfactant, cethyltrimethyl ammonium bromide, occurred between 230 and 290 °C. Moreover, Karthik et al. [43] also associated this weight loss to the decomposition of organic template which was bound within the framework loosely. The final weight loss was seen between 400 and 500 °C. Karthik et al. [43] also observed a fourth peak in their work at 390 °C. They attributed this weight loss to the template cation which was bonded with the metallosilicate framework strongly. They indicated that this temperature was supposed to be increased as the metal loading was increased. By the way, as supported by different studies such as that of Girardon et al. [35,36] the decomposition of cobalt nitrate anions was also endothermic and recognized at 423 K and favoring the formation of Co_3O_4 crystallites. To sum up, 550 °C was found to be suitable as a calcination temperature to remove template completely and to convert cobalt species to Co_3O_4 as a result of decomposition of cobalt nitrate.

The low angle XRD analyses were made between 1° and 10° for the synthesized catalysts and they showed similar diffraction lines for all the materials giving a peak at a 2θ value of about 1.9° (Fig. 2a). This peak was not as sharp as it would be expected for pure MCM-41 and extended upto 2θ values of 10°. In the case of MCM-41 which is a mesoporous material with hexagonally ordered pore structure a characteristic Bragg peak at a 2θ value of 2.30° and its reflections at 3.90°, 4.47° and 5.90° are expected [44]. The catalysts synthesized in the present study were prepared applying modified procedures as for pure MCM-41 [45]. In our case, cobalt and promoter addition was achieved during the one-pot synthesis procedure. High intensity broad peak observed at a 2θ value of 1.90° in the low angle XRD analysis corresponds to the characteristic d_{100} peak of MCM-41. Broadening of this peak and disappearance of the reflection peaks indicated that the addition of cobalt precursor resulted in some deformation in the long range ordered of this structure. A broad peak was observed at 2θ values of 20–30° for all the synthesized catalysts corresponding to the amorphous silicate phase (Fig. 2b). In the high angle XRD analyses of CS7, small peaks observed at 2θ values of 30.24°, 36.44°, 43.10°, 58.40° and 64.12° confirmed the reflection peaks associated to (2 2 0), (3 1 1), (4 0 0), (5 1 1) and (4 4 0) planes of Co_3O_4 crystallites, respectively, [46] (Fig. 2b). By using the diffraction line (3 1 1) the crystallite size of Co_3O_4 was found as 12.6 nm. In the literature it was mentioned that formation of cobalt species was highly dependent on the exothermicity of the precursor decomposition [34,47]. Using cobalt nitrate as a precursor favored the formation of Co_3O_4 with an endothermic decomposition [2,34,35,46,47] as seen in the case of CS7. On the other hand, for CS8 and CS9 catalysts, broad peaks at 2 theta values in the range of 32–38° and 57–62° were observed, showing a shift in diffraction lines with respect to the corresponding Co_3O_4 reflections. It was considered that, for these higher cobalt loading catalysts, cobalt silicate species could be formed and resulted in a shift from Co_3O_4 diffraction lines but it was difficult to distinguish the cobalt silicate only using XRD analysis which was also mentioned by Martinez et al. [33] and Puskas et al. [38].

XPS analyses of the synthesized catalysts showed that the binding energies of Si 2p and O1s lines were in agreement with the literature given for SiO_2 [27]. In the Co 2p XPS spectra of calcined CS7, CS8 and CS9, presented in Fig. 3, Co $2p_{3/2}$ binding energies of 781.7, 782 and 782.6 eV with weak shake up satellites were observed, respectively. In the Co 2p XPS spectra for spinel Co_3O_4,

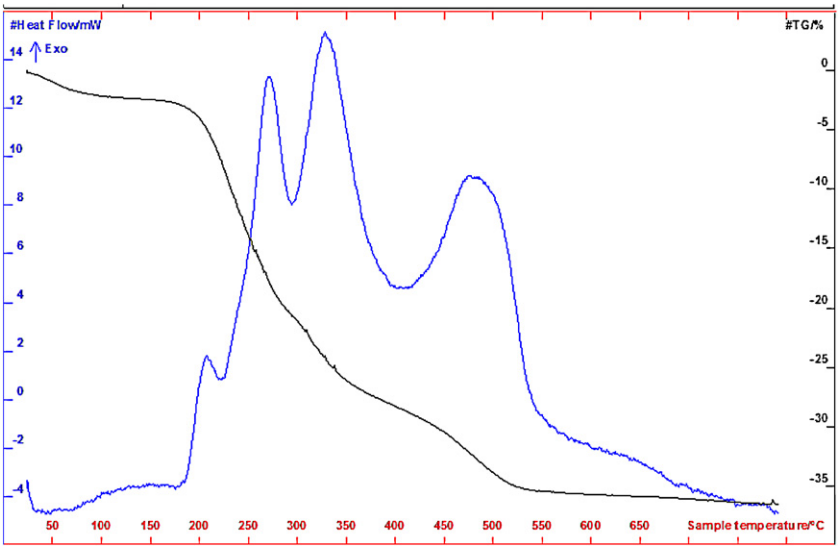

Fig. 1. TGA analysis of uncalcined cobalt based mesoporous silicate.

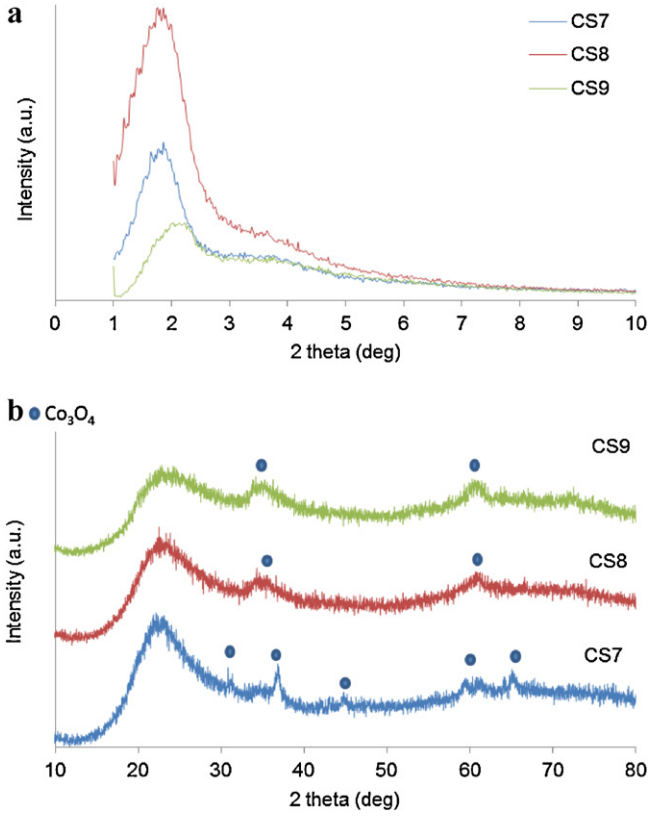

Fig. 2. (a) Low angle (b) high angle XRD profiles of synthesized catalysts.

contribution of Co^{+3}, Co^{+2} and Co^{+2} satellites and their binding energies were reported by Ernst et al. [26]. Co $2p_{3/2}$ binding energies were reported as 780.4 eV for Co^{+2} with a low intensity shake-up satellite peak at about 787.3. A shift of Co $2p_{3/2}$ peak towards to the higher energies and the increase in the relative intensity of shake-up satellite peak were indicated as the presence of Co^{+2} species in octohedral symmetry as found in CoO. This was considered as the strong interaction of cobalt species with the surface of silicate support probably in the form of cobalt silicate [29,32,33,36,37,39]. The XPS spectra of CS7 had a slightly higher Co $2p_{3/2}$ electron binding energy than that of Co_3O_4. It could be explained with a weak interaction between oxide species and silica, as discussed by Ming et al. [39]. It seems that there is limited amount of Co cations incorporated into the framework of mesoporous silica, while there is a large fraction of Co_3O_4 nanoparticles in the matrix of silica which can be supported by the Co_3O_4 peaks in XRD. In the case of CS8 and CS9, higher energy of the Co 2p XPS line and the intense

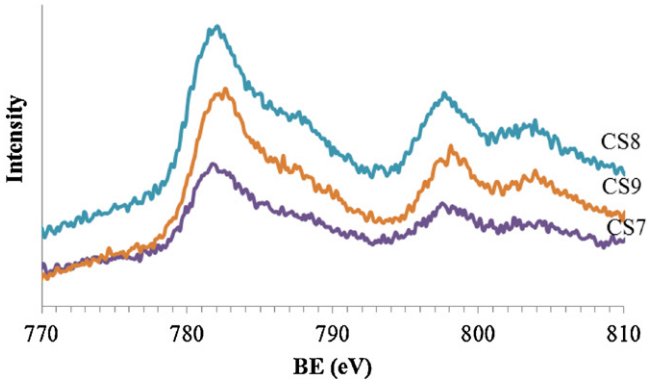

Fig. 3. Cobalt 2p XPS spectra of the synthesized catalysts with promoter.

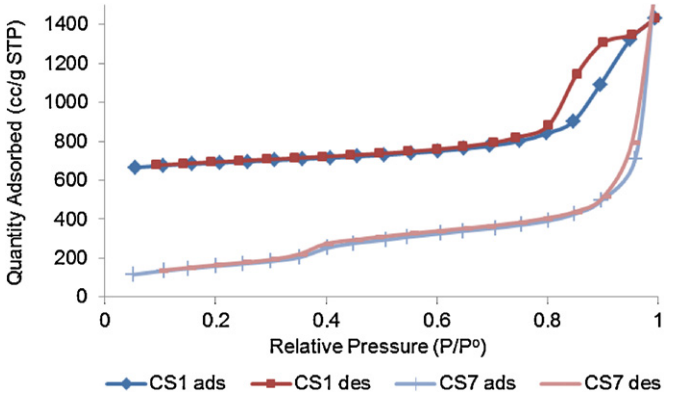

Fig. 4. Nitrogen adsorption–desorption isotherms of CS catalysts with/without promoter (CS1: with KOH, CS7: without KOH, silicate source: TEOS, Co/Si molar ratio: 0.05).

satellite structure were observed. At higher Co contents, the shift in the diffraction peaks with respect to those of Co_3O_4 could be explained with the formation of cobalt silicate. Khodakov et al. [34] and Girardon et al. [35] suggested that the octahedrally coordinated Co^{+2} complexes could either agglomerate into the small crystallites of Co_3O_4 or react with silica yielding the formation of α-cobalt silicate during the oxidative decomposition the cobalt precursor. Reinikainen et al. [27] and Puskas et al. [38] indicated the formation of cobalt silicates during the calcination of the Co/SiO_2 catalysts prepared under the alkaline conditions. Girardon and co-workers also interpret this result in terms of electrostatic attraction between Co^{+2} ions and the silica surface. At a pH value higher than the point of zero charge, which was discussed later on, certain attraction was expected between cobalt ions and negatively charged silica surface. To sum up, at a higher Co content, especially at the Co/Si molar ratio being 0.10–0.15, there could be an interaction between the silicate surface and the cobalt ions resulting the formation of cobalt silicate species which was supported by a shift in the diffraction peaks of CS8 and CS9 with respect to those of Co_3O_4.

On the other hand, peaks corresponding to cobalt or cobalt oxide crystallite were not observed in the XRD patterns of CS1-CS5 catalysts prepared in this work. This result indicated that incorporated Co was very well dispersed and the crystallite size was smaller than the detection limits of XRD. In addition, the Co species that cannot be observed in the XRD patterns could also be the result of cobalt silicate formation.

The nitrogen adsorption–desorption isotherms of the synthesized catalysts were all Type IV according to IUPAC classification, indicating mesoporous structure which was supported by the TEM analyses of the synthesized catalysts. A summary of physical and chemical properties of the catalysts is given in Table 1. Isotherms corresponding to CS1 and CS7, presented in Fig. 4, were the typical examples to the catalysts prepared without and with promoters, respectively. These isotherms showed some distinct differences. The only difference of the synthesis procedures of these two catalysts is the addition of KOH during the synthesis of CS7. From the EDX analyses, the molar ratio of K/Co in the synthesized catalysts was found about 0.04. For CS1, capillary condensation took place at P/P^0 value of about 0.80–0.95 and in the case of CS7 capillary condensation in the mesopores took place at P/P^o close to 0.40. These values correspond to pore diameters of about 17 nm and 3.1 nm, respectively. Significant increase in surface area and pore volume was also observed as a result of KOH addition to the synthesis solution (Table 1).

Another observation made from the N_2 adsorption–desorption analysis is the increase of average pore diameter and pore volume with a decrease in surface area as a result of increase of Co loading.

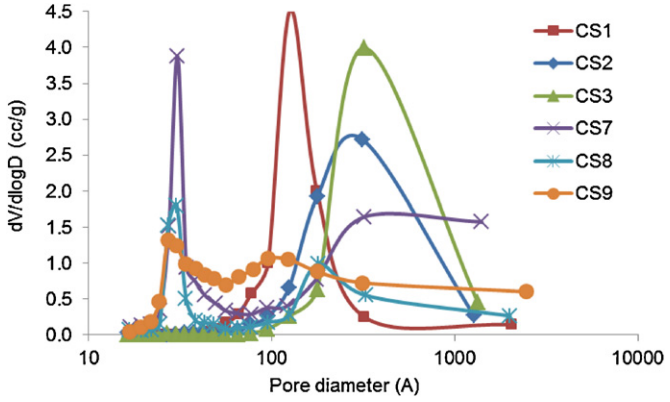

Fig. 5. Pore size distributions of CS catalysts with/without promoter (silicate source: TEOS).

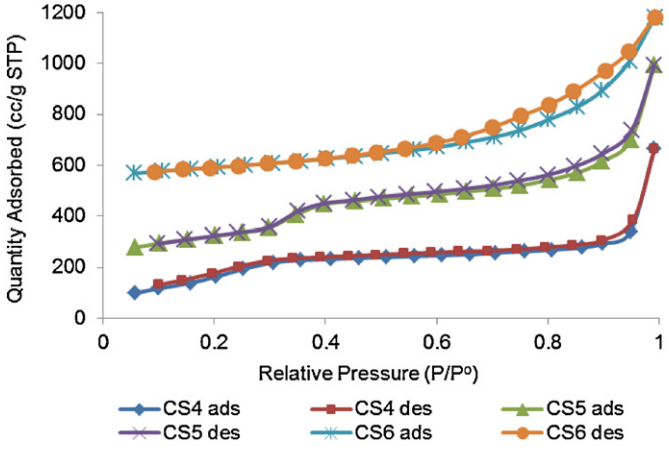

Fig. 6. Nitrogen adsorption–desorption isotherms of CS4, CS5 and CS6 catalysts.

As given in Table 1, while the pore volume of CS1 was 1.29 cc/g, it was 1.45 and 1.71 cc/g for CS2 and CS3, respectively. Multiple point BET surface area values of CS1, CS2 and CS3 were found as 317, 228 and 192 m^2/g, respectively, showing a decrease due to an increase in Co content of the catalysts. The hysteresis loops seen in the isotherms of CS1 were classified as H2 type. This type of hysteresis was explained with the Network model which could be due to the interconnectivity of the porous network [48]. Santos et al. [46] also discussed H2 type hysteresis observed in their N_2 adsorption desorption isotherms of silica cobalt composite materials and explained with the typical behavior of amorphous materials having pores with ink pot geometry.

Typical pore size distributions of the synthesized materials are shown in Fig. 5. The results showed that CS1 had a narrower pore size distribution than CS2 and CS3. While the average pore diameter of CS1 was 16.9 nm, CS2 and CS3 had an average pore diameter values of 29.5 and 32.0 nm, respectively. So, the pore size distribution curves became wider and shifted to the higher pore diameter values with the increase in cobalt loading. The adsorption and desorption branches of the catalysts prepared with promoter KOH nearly parallel to each other indicating Type H1 hysteresis as in the case of CS7 presented in Fig. 4. A narrow pore distribution was seen in a pore diameter range between 2 and 6 nm for this material (Fig. 5). Due to the extension of pore size distribution, a plateau did not exist in the adsorption–desorption isotherms of CS7, CS8 and CS9 catalysts [49]. Although the Co/Si molar ratio in the synthesis solution was adjusted in the same interval (0.05–0.15) for both group of catalysts using the same silicate source (TEOS), the pore size diameters of CS7-CS9 were much lower than that of CS1-CS3 while the surface area values of the former ones were higher than that of latter ones. These results were obtained due to the addition of KOH. In the literature, alkali promoters were evaluated in ammonia decomposition reaction with different catalysts and the effects of KOH were summarized like that (a) increasing dispersion which resulted in formation of small crystallites [17], (b) modifying the basicity of the support material [3], (c) preventing the sintering of the active metals [4]. Moreover studies showed that effects of potassium promoter mainly dependent on the metal and the support used in the preparation of catalyst [3,4].

Nitrogen adsorption–desorption isotherms of the materials prepared by using sodium silicate (instead of TEOS) as the Si source are shown in Fig. 6. The behavior of hysteresis in the nitrogen adsorption–desorption isotherms of the catalysts containing different Co loadings showed some differences. The adsorption and desorption branches of CS4 and CS5 were found to be nearly coincidence to each other which could be seen typically for highly ordered cylindrical mesoporous material as in the case of CS7. TEM images presented in Fig. 7a and b showed the well-ordered hexagonal arrangement of the channels perpendicular and parallel to the *c* axis in the structure of CS4 and CS5, respectively. The small dark points seen in hexagonal structures and the contrast seen in the longitudinal axis were the indications of the cobalt oxides present inside the pores and this statement was supported by the EDX analysis. A very familiar TEM image of mesoporous Co/SBA catalysts prepared by impregnation procedure was recognized and the smeared contrast, which was also observed in very limited locations in CS4 and CS5 structure, was indicated as the cobalt particles located on the external surface by Martinez et al. [33]. The type of hysteresis loop for CS6, which contained the highest cobalt loading among them, occurred in the relative pressure (P/P^0) range between 0.6 and 1.0, but this loop was not terminated in a plateau. It was classified as type H3 according to IUPAC classification and it was explained with the aggregates of platy particles or adsorbents having slit-shaped pores [50,51]. TEM images presented in Fig. 7c showed the effect of higher cobalt loading on the catalyst texture. CS4, containing the lowest amount of Co, has a high surface area around 839 m^2/g and has a very narrow pore size distribution in the range of 1.7–4.2 nm with an average value of 2.2 nm, calculated from BJH adsorption data (Fig. 8). A decrease in surface area with an increase in cobalt loading was observed as given in Table 1. CS6 which had the smallest surface area showed a very broad pore size distribution ranging from 2.2 to 29.5 nm (Fig. 8). This material also contained some micropores. These results showed that the source of Si and the Co loading had significant effect on the structural properties of the synthesized mesoporous materials. Although CS1-CS3 and CS4-CS6 catalysts prepared adjusting the same Co/Si molar ratio in the synthesis solution (Table 1), for example both of CS1 and CS4 contained cobalt precursor at Co/Si molar ratio of 0.05, by using different silicate sources, their surface area and pore size diameters were highly different from each other. The pH of the synthesis solution was also quite different depending on the silica sources. While highly acidic pH value was measured in the synthesis solution contained TEOS, it was around 11 in the case of sodium silicate.

In the EDX analyses of the catalysts prepared using TEOS without promoter, Co/Si molar ratio was found to be lower than the values adjusted in the final synthesis solutions. For instance Co/Si ratio evaluated from EDX analysis of CS1 was about 0.02, while this ratio was 0.05 in the synthesis solution. The pH of the final synthesis solution was around 3.8 for these catalysts. Results proved that Co incorporation was not very successful at the acidic conditions. Similar results in difficulties for incorporation of metals into the structure of mesoporous silica at the acidic conditions were also reported in the literature [52,53]. Girardon et al. [36] indicated that the point of zero charge for silica correspond to the pH value in the range of 2–3.5. Above these values silica take a

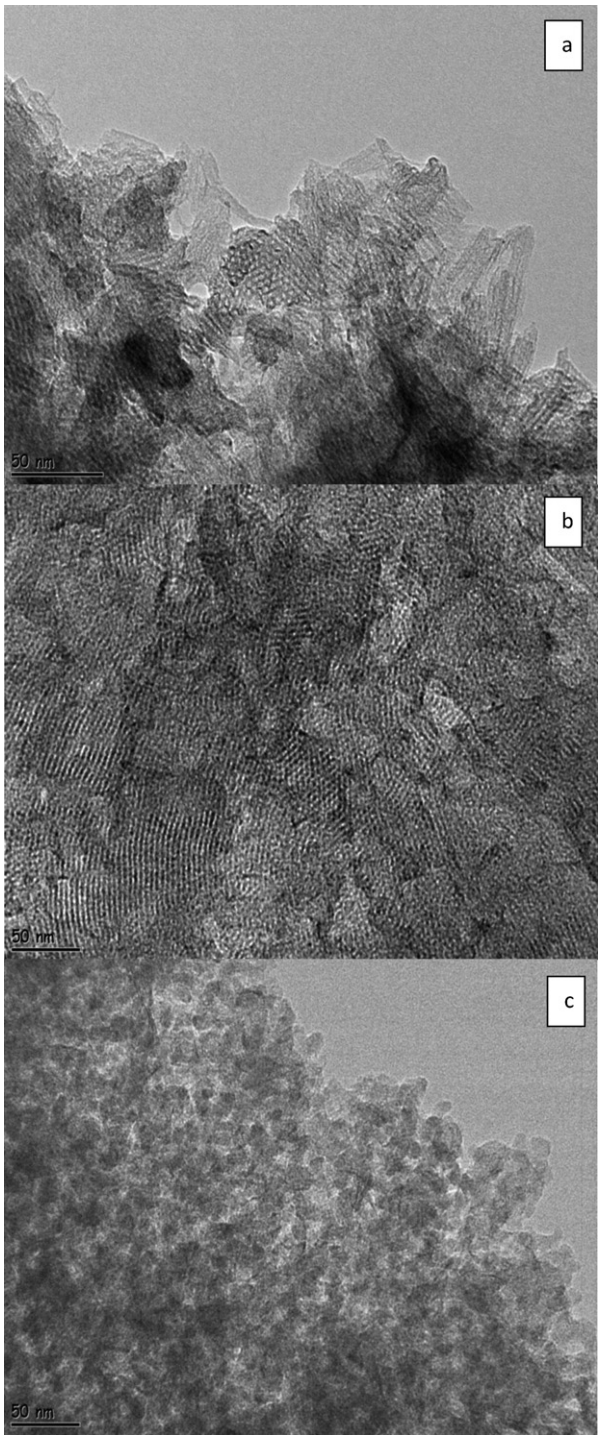

Fig. 7. HRTEM images of (a) CS4, (b) CS5 and (c) CS6 catalysts.

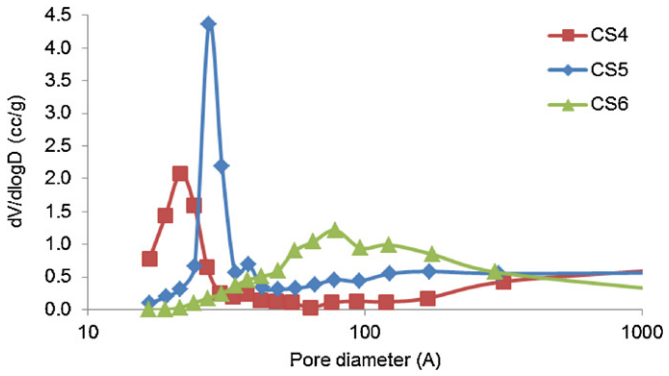

Fig. 8. Pore size distributions of CS4, CS5 and CS6 catalysts.

negative charge and the possibility of cobalt dispersion might be increased. The pH of the final synthesis solution of CS1, CS2 and CS3 was slightly higher than the point of zero charge level, so adsorption of the positively charged cobalt ions on silica was expected to occur. Liou et al. [54] mentioned the electrostatic interaction occurred between the charged silica particles and surfactant templates in their work on the preparation of MCM-41 in acidic and alkaline environment. Highly acidic environment in which negatively charged silica interacted with positively charged surfactant and highly basic environment in which cationic silica interacted with surfactant by counterion-mediated binding, were found very suitable for the formation of hexagonally ordered mesoporous structure [49,54]. For the pH values between these two extreme cases some deformations were proposed in the ordered mesoporous structure. Actually, this situation may support the results retrieved from the XRD and nitrogen physisorption analyses of CS1, CS2 and CS3 catalysts. Mesoporous structure with some deformation was obtained due to the presence of cobalt in the synthesis solution. However the pH of the solution is not very appropriate and limited amount of cobalt remains in the structure.

The Co/Si molar ratios of the materials synthesized at the basic conditions using sodium silicate as the Si source were also evaluated by EDX analysis. Co/Si ratios of CS4, CS5 and CS6 were found as 0.056, 0.093 and 0.12, respectively from EDX analysis. These values were quite close to the corresponding ratios in the synthesis solution. As indicated in experimental part, the pH of the synthesis solution was adjusted to 11 and it was not changed much after the addition of cobalt nitrate. Results showed that at this pH level incorporation of cobalt into the mesoporous silicate structure was favored as supported by the TEM images presented in Fig. 7. Higher surface area with narrow pore size distribution values were obtained for CS4-CS6 catalysts in comparison to CS1-CS3 catalysts. Highly basic synthesis solution could be an important reason of this situation.

The pH of the final synthesis solution of CS7-CS9 catalysts was around 8 which was lower than that of CS4-CS6 catalysts but higher than that of CS1-CS3 catalysts. According to the knowledge obtained from Girardon et al. [36] and Liou et al. [54]; this pH is also convenient for obtaining mesoporous structure with the interaction of negatively charged silica and positively charged surfactant. A lower surface area was expected due to the lower density of negatively charged silica in this pH value comparing to the more basic one. Nitrogen physisorption analyses supported this statement, i.e. BET surface area of CS7 was around 577 m^2/g while BET surface area of CS4 was 741 m^2/g. On the other hand BET surface area of CS1 was 317 m^2/g. The Co/Si molar ratio obtained from EDX analyses was very close to the value adjusted in the synthesis solution such as 0.055 was retrieved for CS7 (0.05 in the synthesis solution). Mesoporous structure with good cobalt dispersion was also seen in the TEM images of the catalysts prepared with promoter (Fig. 9). When the results of CS1-CS3 and CS7-CS9 catalysts are compared, effective promoting effects of KOH are clearly seen. Better incorporation and distribution of cobalt throughout the silicate structure which is more likely due to the pH of the synthesis solution in CS7 in comparison to CS1 are also seen in Fig. 10.

The difference in the size of the CS1-CS3 and CS7-CS9 catalysts was seen in their SEM analyses. Particles having a uniform distribution of 50 nm in dimensions were observed for CS7 catalyst while larger particles which were around 250 nm were observed for CS3 catalyst.

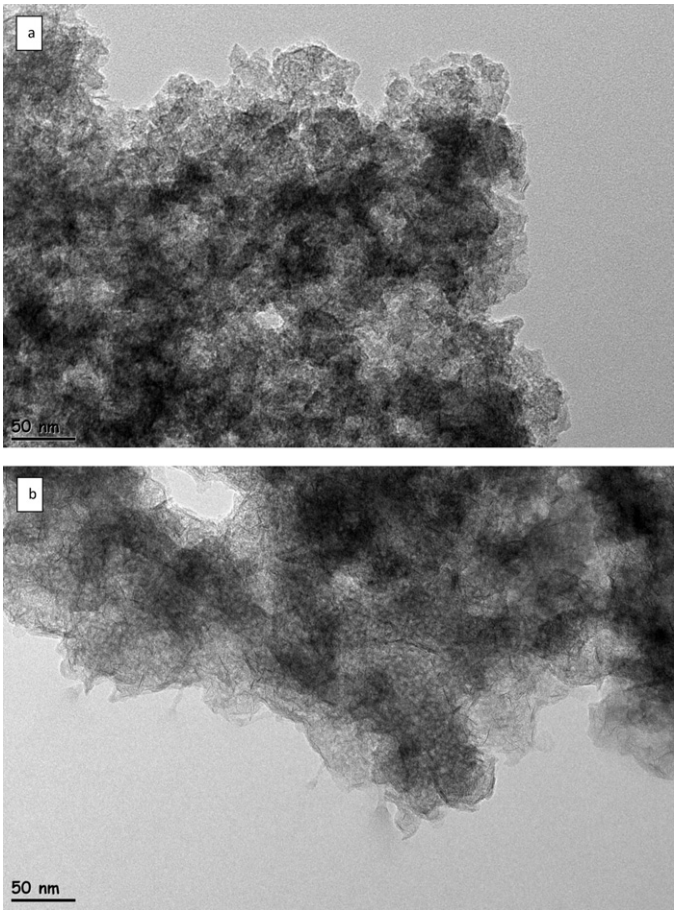

Fig. 9. HRTEM images of (a) CS8 and (b) CS9 catalysts.

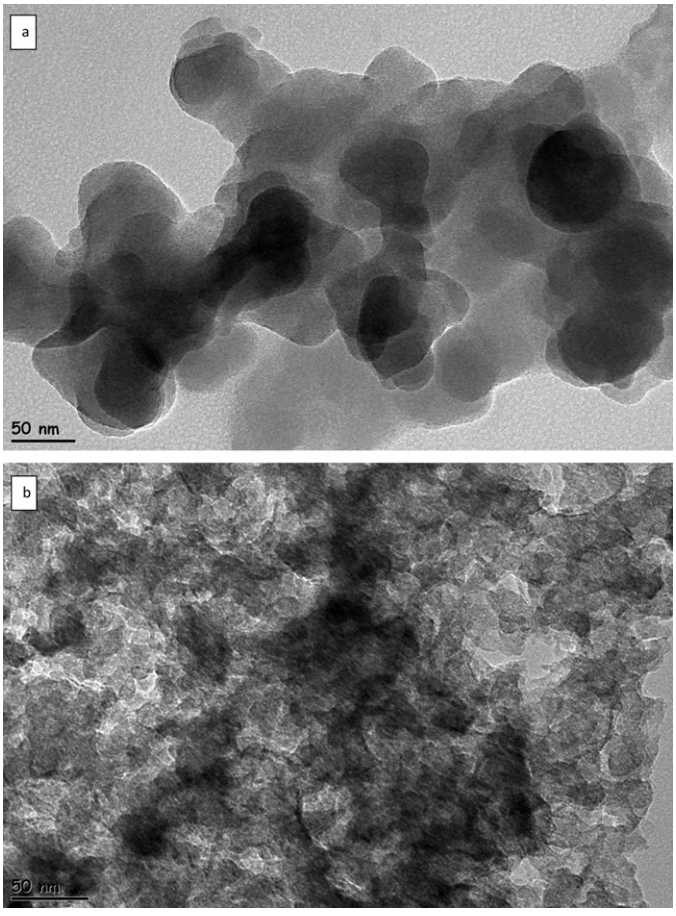

Fig. 10. HRTEM images of (a) CS1 and (b) CS7 catalysts.

3.2. Catalytic activity results

Experimental results of ammonia decomposition reaction over CS1, CS2 and CS3 catalysts, using pure ammonia with a feed flow rate of 250 ml/min are presented in Fig. 11a. Up to the reaction temperature of 600 °C, catalytic activities of these catalysts were negligible. At around 600 °C, the conversion values of CS1 and CS3 were 6.5% and 1.3%, respectively, whereas that of CS2 reached to 18.7%. Increasing reaction temperature enhanced conversion values for these catalysts. For instance, ammonia conversion values of 29 and 82% were obtained at 700 °C over CS3 and CS2, respectively. Experiments were carried out up to 750 °C and at this temperature approximately 94% conversion was obtained with CS1 and CS2. For all the studied reaction temperatures, activity of CS3 catalyst was lower than the activity obtained with the other catalysts. In spite of lower cobalt loading of CS1 than that of CS3, the former's better activity could be explained with the better distribution of metal through amorphous silicate structure. The overall surface area could not be considered as the determinable factor for the activity. For example, activity of CS1 was lower than the activity of CS2 even though CS1 had the highest surface area among the catalysts in this group, as seen in Fig. 11a and Table 1. This is because the contribution of surface area of SiO_2 itself to the activity should be rather small. This situation indicates that the key factor is actually the form and dispersion of Co oxide in the SiO_2 phase and, very importantly, the accessibility of these Co species in the samples as discussed in the literature [25,28]. Among these catalysts, CS2 was much better than the others since it showed higher activity at lower reaction temperatures.

Catalytic activities of CS4-CS6 catalysts, which were prepared by using sodium silicate, at different reaction temperatures, were presented in Fig. 11b. As in the case of CS1-CS3 catalysts, CS4-CS6 catalysts showed negligible activity up to 600 °C. When the temperature reached to 600 °C, CS5 catalyst showed 50% ammonia conversion while CS4 and CS6 showed approximately 15% ammonia conversion under the same reaction conditions. CS5, which contained cobalt in a Co/Si molar ratio of 0.10, showed even some activity at 500 °C. Activity of CS5 was found much higher than the activity of CS2 which was prepared using TEOS at acidic conditions. These results indicate that the catalytic activity is related to the texture and porosity of the SiO_2 matrix which is actually associated to the accessibility of the Co species. In the literature it was also indicated that periodic mesoporous silicas were likely to facilitate the distribution and stabilization of cobalt particles and to prevent them from sintering [30,33]. As seen in Figs. 8 and 7b, ordered mesoporous structure of CS5 enables the better distribution of cobalts. These results proved that dispersion of Co greatly enhanced the catalytic performance of the synthesized catalysts. Increase in temperature resulted in an increase in ammonia conversion, as it would be expected. Close to total conversion was achieved at 700 °C over CS5 catalyst.

Better performance of CS4-CS6 catalysts in ammonia decomposition reaction in comparison to CS1-CS3 catalysts presented in Fig. 11a and b, respectively, indicated that the synthesis conditions enhanced the texture and the porosity of the SiO_2 matrix associated with the incorporation of cobalt and the accessibility of cobalt species.

As shown in Fig. 11c, all of the synthesized catalysts with KOH promoter have the activities over 50% at a reaction temperature

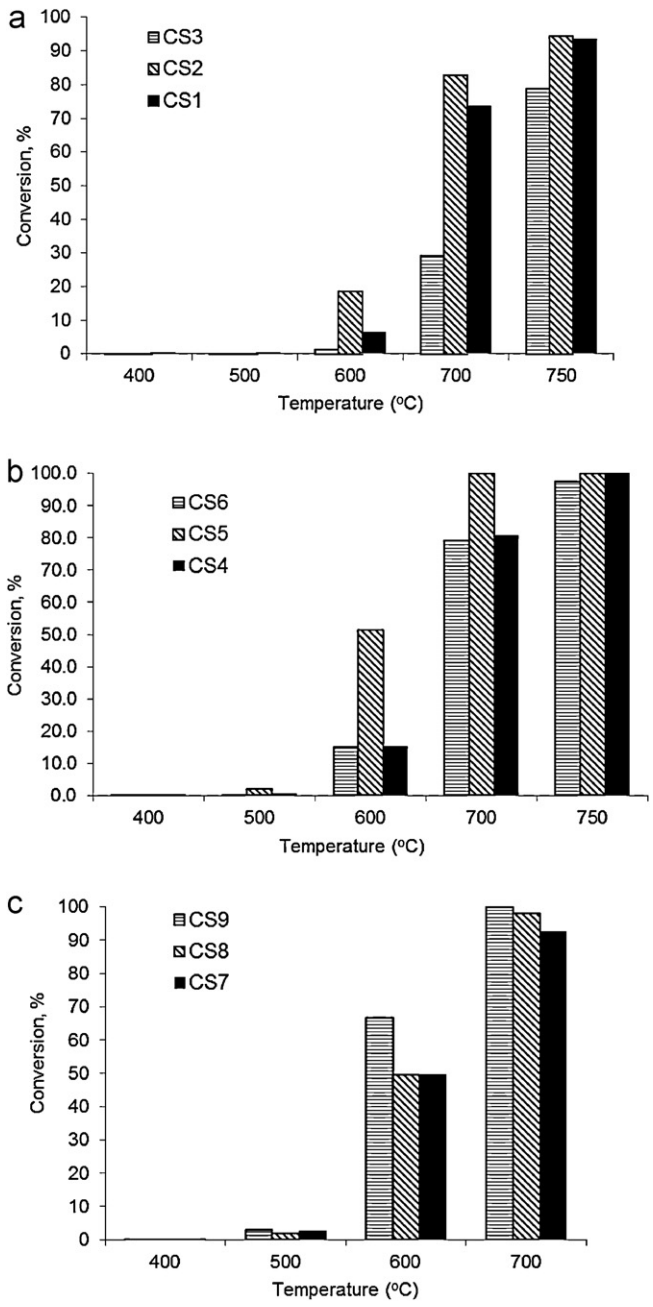

Fig. 11. Conversion of ammonia over (a) CS1-CS3, (b) CS4-CS6, (c) catalyst with promoter, at different reaction temperatures, $Q_{NH_3,inlet}$ = 250 ml/min, $m_{catalyst}$: 0.1 g.

of 600 °C. In fact, approximately 70% conversion was obtained over CS9 catalyst. On the other hand, under the same reaction condition the maximum ammonia conversion was only 18% which was obtained by CS2. When the reaction temperature increased to 700 °C, 92%, 98% and close to total ammonia conversion was obtained with CS7, CS8 and CS9, respectively. These results showed that the addition of KOH as a promoter greatly enhanced the catalytic activity of the catalysts which was also supported by the work of Yin et al. [3]. The differences in the texture and the porosity of the catalysts prepared without promoter and with promoter were clearly seen in pore size distribution curves presented in Fig. 5 and the corresponding TEM images presented in Fig. 10. Activity results proved that better accessibility of the Co species occurred with the addition of KOH.

As described in the experimental part, all of the synthesized catalysts were in situ reduced before being tested in ammonia

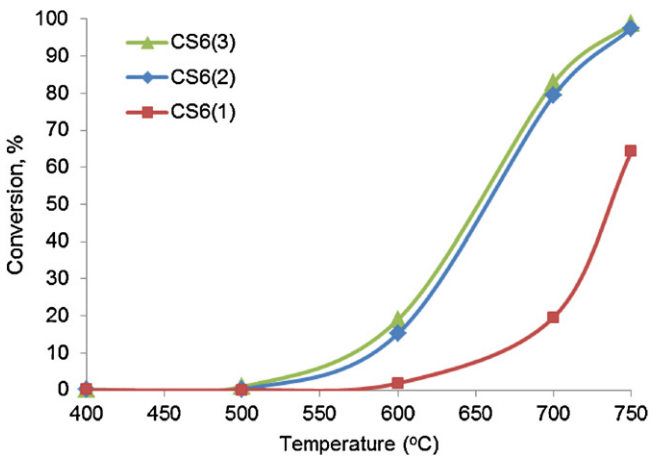

Fig. 12. Conversion of ammonia over CS6 reduced at 400 °C for different time duration, $Q_{NH_3,inlet}$ = 250 ml/min, $m_{catalyst}$: 0.1 g.

decomposition reaction. Literature related on the application of cobalt based silicate catalysts in ammonia decomposition reaction is very rare. For this reason, in order to get high activity from the synthesized catalysts, it was decided to determine the optimum reduction time interval by comparing the results of experiments which were carried out with one of the catalysts reduced at the same temperature for different durations. CS6 was selected for this comparison and it was in situ reduced at 400 °C under the flow of pure hydrogen (60 ml/min) for 60, 120 and 180 min intervals and these catalysts were denoted as CS6(1), CS6(2) and CS6(3), respectively. Activity measurements were repeated in a temperature interval of 400–750 °C with pure ammonia feed having a flow rate of 250 ml/min for each case. As shown in Fig. 12, when the reaction temperature was higher than 500 °C, CS6(2) and CS6(3) showed higher activity than CS6(1). As the reaction temperature was increased to 600 °C and then 700 °C, the same trend was followed by CS6(2) and CS6(3) reaching to approximately 20% and 80% conversion respectively. On the other hand CS6(1) gave only 2% conversion at 600 °C and 20% at 700 °C. According to these results, reduction for 60 min was not enough, meanwhile conversion values were not so much different for the catalysts reduced for 120 or 180 min. So, reduction at 400 °C under the flow of pure hydrogen for 120 min was found to be sufficient for the synthesized cobalt based mesoporous catalysts in ammonia decomposition experiments.

Catalytic activity of the cobalt based mesoporous silicate catalysts reduced at a temperature higher than 400 °C was investigated by using CS5 catalyst being reduced at 500 °C for 2 h. Ammonia decomposition reaction experiments were performed under the same conditions described as before. The results were presented in Fig. 13 comparing with the results obtained over CS5 reduced at 400 °C. When the reaction temperature was 500 °C catalytic activity was negligible for both cases. At a reaction temperature of 600 °C ammonia conversion of 51% was obtained for CS5, which was reduced at 400 °C, while conversion was around 32% for CS5 reduced at 500 °C. When the reaction temperature was increased to 700 °C, about 10% difference was seen between these two conditions. Reduction temperature is known to change the oxidation state of Co. In the study of Song and Ozkan [2], on phase transformation of standard Co_3O_4 it was found that at a reduction temperature of 350 °C Co_3O_4 phase disappeared and CoO phase appeared. Reduction of Co_3O_4 at 345 °C was also mentioned by Santos et al. [46] in their TPR study of the synthesized silica cobalt composites prepared with cobalt nitrate salt. Song and Ozkan [2] also mentioned that when the reduction temperature became higher than 400 °C CoO phase disappeared and metallic Co phase appeared at 450 °C. In an earlier study, Martinez et al. [33]

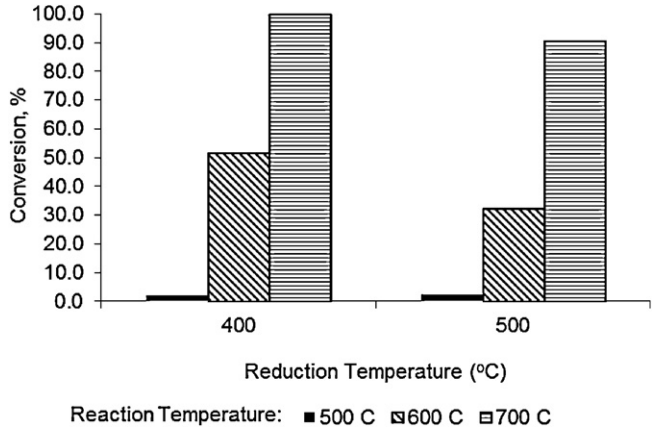

Fig. 13. Conversion of ammonia over CS5 reduced at different temperature for 2 h, $Q_{NH_3,inlet}$ = 250 ml/min, $m_{catalyst}$: 0.1 g.

also reported reduction of supported Co_3O_4 crystallite to CoO at temperatures below 673 K and reduction to metallic Co at higher temperatures. Due to the metal support interaction these transformations were said to be occurred at higher temperatures [2]. For example, for the nanosized Co_3O_4 solid, lower reduction temperatures were reported, i.e. reduction of Co^{+3} to Co^{+2} and the formation of CoO occurred at 260 °C and the reduction of CoO to metallic cobalt occurred at 322 °C [46]. After the reduction of CS5 catalyst at 400 °C, CoO was supposed to be formed. With the increase in reduction temperature to 500 °C, metallic Co phase was expected in the structure. Considering the activity results CoO phase may be favorable in ammonia decomposition reaction, however, the reaction temperatures were much higher than 400 °C and both Co_3O_4 and CoO were expected eventually transformed into metallic Co in the hydrogen rich atmosphere during reaction indicating activity of the metallic cobalt. These results reveal that reduction at 400 °C is sufficient for getting active species in the synthesized cobalt incorporated silicate structured catalysts for ammonia decomposition reaction.

Some experiments were also performed at different space velocity (Fig. 14). For this purpose, ammonia decomposition reaction was tested using the same amount of catalyst with a different feed flow rate other than 250 ml/min. Experiments were performed in a temperature interval of 400–700 °C over the catalyst CS5, which was in situ reduced at 400 °C. Pure ammonia was feed to the system at a flow rate of 60 ml/min. At 700 °C there was not seen change in ammonia conversion with feed flow rate, i.e. almost total conversion of ammonia took place over CS5. On the other hand at

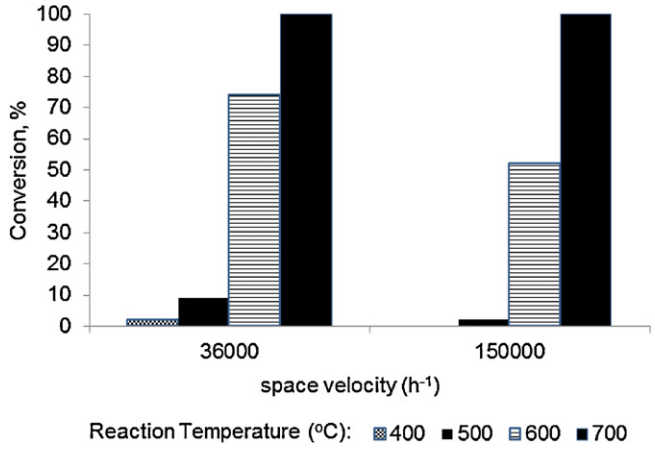

Fig. 14. Conversion of ammonia over CS5 at different space velocity, $m_{catalyst}$: 0.1 g.

Table 2
Overall hydrogen production rate per gram of catalyst (mmol/min $g_{catalyst}$) at different reaction temperatures ($Q_{NH_3,inlet}$ = 250 ml/min).

Catalyst	400 °C	500 °C	600 °C	700 °C
CS1	0.09	0.19	10.05	112.70
CS2	0.08	0.82	30.14	133.60
CS3	0.04	0.04	1.74	39.82
CS4	0.22	0.38	21.56	113.79
CS5	0.23	2.88	72.77	140.96
CS6	0.05	0.29	18.69	97.30
CS7	0.46	4.95	91.22	170.05
CS8	1.02	3.16	91.15	180.49
CS9	0.12	4.31	102.50	153.36

a temperature interval of 500–600 °C, using lower feed flow rate resulted in higher ammonia conversion. Change of flow rate from 250 ml/min to 60 ml/min caused a decrease in space velocity from 150,000 h^{-1} to 36,000 h^{-1}. Obtaining 74% conversion at 600 °C at a space velocity of 36,000 h^{-1} (over CS5) was a highly promising.

When the equilibrium conversion values were calculated at 1 atm for different reaction temperatures it was seen that, at 400 °C the equilibrium conversion value for ammonia decomposition reaction was over 99%. This result indicated that there was no equilibrium limitation in the reaction temperature interval studied in this work.

The overall hydrogen production rate per gram of catalyst at different reaction temperatures was evaluated and reported in Table 2. Results showed that the activity of the KOH promoted CS7, CS8 and CS9 group of catalysts was higher than that of the other catalysts. The overall hydrogen production rate per gram of catalyst was around 3–5 mmol/min $g_{catalyst}$ at 500 °C and it increased to 90 mmol/min $g_{catalyst}$ at 600 °C. The catalytic activity of CS5 was also tested at a feed flow rate of 60 ml/min and it gave overall rate values of 27.10 mmol/min $g_{catalyst}$ and 36.81 mmol/min $g_{catalyst}$ at 600 °C and 700 °C, respectively. In the work of Choudhary et al. [10], hydrogen formation rates at 600 °C with a feed flow rate of 50 ml/min over Ni/SiO_2, Ir/SiO_2 and Ru/SiO_2 were reported as 11.4, 17.6 and 30.3 mmol/min g_{cat}, respectively. These catalysts were prepared by wet impregnation procedure using ordinary silica as the support with 10% metal loading. In the case of MCM-41 and SBA-15 supported Ni catalysts, higher hydrogen formation rates (21.5 and 19.2 mmol/min g_{cat} respectively) were reported at the same temperature and feed flow rate [4]. It was also seen that mesoporous silicate encapsulated Fe_2O_3 catalysts gave hydrogen formation rate changing between 25.78 and 26.18 mmol/min g_{cat} while the Cs modified ones gave hydrogen formation rate in between 28.06 and 30.30 mmol/min g_{cat} under the same conditions [20]. These results showed that the synthesized catalysts were highly promising in ammonia decomposition reaction.

4. Conclusions

Cobalt based mesoporous silicate catalysts were prepared by using one-pot hydrothermal synthesis procedure. Catalysts prepared by using sodium silicate had a well ordered mesoporous structure with a higher surface area and narrower pore size distribution compared to the catalysts prepared by using TEOS. These results proved the importance of synthesis solution pH on the structure of the final product. Incorporation of cobalt was better for the former case; this could be explained with the basic pH of the final synthesis solution. For all the catalysts, increasing cobalt loading resulted in lower surface area. Results showed that catalyst prepared with KOH promoter had higher surface area and lower pore diameters compared to the ones without promoter. In addition, presence of KOH greatly enhanced the incorporation of cobalt into the mesoporous lattice of the amorphous silica.

Higher pH value of the synthesis solution is the possible reason of this observation. Co_3O_4 crystallite was expected to form after the calcination of catalysts prepared by using cobalt nitrate at 550 °C. At higher Co content, especially at the Co/Si molar ratio being 0.15, there can be certain amount of cobalt silicate species formed in the sample which can be supported by the shift in the diffraction peaks with respect to those of Co_3O_4. Generally Type IV adsorption desorption isotherms, indicating mesoporous structure of the catalysts, were seen with different hysteresis types. All of the cobalt based mesoporous silicate catalysts showed activity in ammonia decomposition reaction at temperatures higher than 500 °C. The form and the dispersion of Co oxide in SiO_2 matrix and, very importantly, the accessibility of these Co species in the samples which is in turn related to the texture and porosity of the SiO_2 matrix affected the catalytic activity. Using pure ammonia feed with a space velocity of 150,000 h^{-1} close to complete conversion was obtained between 700 and 750 °C. Among the synthesized catalysts the ones prepared with KOH promoter gave the highest activity i.e. ammonia conversion of 70% was obtained at 600 °C over CS9. Prior to the experiment, fresh catalyst was reduced in situ at 400 °C under the flow of pure hydrogen for 2 h. Reduction time interval of 2 h was found to be sufficient since ammonia conversion values did not change significantly with the catalysts reduced at 400 °C for longer periods. An increase of ammonia conversion from 52% to 74% by decreasing the space velocity from 150,000 h^{-1} to 36,000 h^{-1} over catalyst CS5 at 600 °C was found to be highly promising.

Acknowledgment

This study was financially supported by TUBITAK through Project No. 109M560 Project and Gazi University Research Fund through Project No.18-2010/07. They are gratefully acknowledged.

References

[1] A.S. Chellappa, C.M. Fischer, W.J. Thomson, Applied Catalysis A 227 (2002) 231–240.
[2] H. Song, U.S. Ozkan, Journal of Molecular Catalysis A: Chemical 318 (2010) 21–29.
[3] S.F. Yin, Q.H. Zhang, B.Q. Xu, W.X. Zhu, C.F. Ng, C.T. Au, Journal of Catalysis 224 (2004) 384–396.
[4] X.K. Li, W.J. Ji, J. Zhao, S.J. Wang, C.T. Au, Journal of Catalysis 236 (2005) 181–189.
[5] Y. Li, S. Liu, L. Yao, W. Ji, C.T. Au, Catalysis Communications 11 (2010) 368–372.
[6] R. Metkemeijer, P. Achard, Journal of Power Sources 49 (1994) 271–282.
[7] A.H. Lu, J.J. Nitz, M. Comotti, C. Weidenthaler, K. Scslichte, C.W. Lehmann, O. Terasaki, F. Schüth, Journal of the American Chemical Society 132 (2010) 14152–14162.
[8] J. Zhang, H. Xu, Q. Ge, W. Li, Catalysis Communications 7 (2006) 148–152.
[9] G. Papapolymerou, V. Bontozoglou, Journal of Molecular Catalysis A: Chemical 120 (1997) 165–171.
[10] T.V. Choudhary, C. Sivadinarayana, D.W. Goodman, Catalysis Letters 72 (2001) 197–201.
[11] S.F. Yin, B.Q. Xu, W.X. Zhu, C.F. Ng, X.P. Zhou, C.T. Au, Catalysis Today 93–95 (2004) 27–38.
[12] M.C.J. Bradford, P.E. Fanning, M.A. Vannice, Journal of Catalysis 172 (1997) 479–484.
[13] K. Hashimoto, N. Toukai, Journal of Molecular Catalysis A: Chemical 161 (2000) 171–178.
[14] W. Rarog-Pilecka, D. Szmigiel, Z. Kowalczyk, S. Jodzis, J. Zielinski, Journal of Catalysis 218 (2003) 465–469.
[15] W. Zheng, J. Zhang, H. Xu, W. Li, Catalysis Letters 119 (2007) 311–318.
[16] R. Pelka, I. Moszynska, W. Arabczyk, Catalysis Letters 128 (2009) 72–76.
[17] A. Jedynak, Z. Kowalczyk, D. Szmigiel, W. Rarog, J. Zielinski, Applied Catalysis A-General 237 (2002) 223–226.
[18] W. Arabczyk, J. Zamlynny, Catalysis Letters 60 (1999) 167–171.
[19] J. Zhang, M. Comotti, F. Schüth, R. Schlögl, D.S. Su, Chemical Communications (2007) 1916–1918.
[20] Y. Li, L. Yao, S. Liu, J. Zhao, W. Ji, C.T. Au, Catalysis Today 160 (2011) 97–105.
[21] S.S. Pansare, J.G. Goodwin Jr., Industrial and Engineering Chemistry Research 47 (2008) 4063–4070.
[22] M.E.E. Abashar, Y.S. Al-Sughair, I.S. Al-Mutaz, Applied Catalysis A 236 (2002) 35–53.
[23] J. Zhang, H. Xu, X. Jin, Q. Ge, W. Li, Applied Catalysis A 290 (2005) 87–96.
[24] W. Rarog-Pilecka, D. Szmigiel, A. Komornicki, J. Zielinski, Z. Kowalczyk, Carbon 41 (2003) 579–625.
[25] E. Iglesia, Applied Catalysis A 161 (1997) 59–78.
[26] B. Ernst, A. Bensaddik, L. Hilaire, P. Chaumette, A. Kiennemann, Catalysis Today 39 (1998) 329–341.
[27] M. Reinikainen, M.K. Niemela, N. Kakuta, S. Suhonen, Applied Catalysis A 174 (1998) 61–75.
[28] B. Ernst, S. Libs, P. Chaumette, A. Kiennemann, Applied Catalysis A 186 (1999) 145–168.
[29] A.Y. Khodakov, A. Griboval-Constant, R. Bechara, V.L. Zholobenko, Journal of Catalysis 206 (2002) 230–241.
[30] A.Y. Khodakov, R. Bechara, A. Griboval-Constant, Studies in Surface Science and Catalysis 142 (2002) 1133–1140.
[31] A. Griboval-Constant, A.Y. Khodakov, R. Bechara, V.L. Zholobenko, Studies in Surface Science and Catalysis 144 (2002) 609–616.
[32] A.Y. Khodakov, R. Bechara, A. Griboval-Constant, Applied Catalysis A 254 (2003) 273–288.
[33] A. Martinez, C. Lopez, F. Marquez, I.J. Diaz, Journal of Catalysis 220 (2003) 486–499.
[34] A.Y. Khodakov, J.S. Girardon, A. Griboval-Constant, A.S. Lermontov, P.A. Chernavskii, Studies in Surface Science and Catalysis 147 (2004) 295–300.
[35] J.S. Girardon, A. Constant-Griboval, L. Gengembre, P.A. Chernavskii, A.Y. Khodakov, Catalysis Today 106 (2005) 161–165.
[36] J.S. Girardon, A.S. Lermontov, L. Gengembre, P.A. Chernavskii, A. Griboval-Constant, A.Y. Khodakov, Journal of Catalysis 230 (2005) 339–352.
[37] J.S. Girardon, E. Quinet, A. Griboval-Constant, P.A. Chenavskii, L. Gengembre, A.Y. Khodakov, Journal of Catalysis 248 (2007) 143–157.
[38] I. Puskas, T.H. Fleisch, J.A. Kaduk, C.L. Marshall, B.L. Meyers, M.J. Castagnola, J.E. Indacochea, Applied Catalysis A 316 (2007) 197–206.
[39] H. Ming, B.G. Baker, M. Jasieniak, Applied Catalysis A 381 (2010) 216–225.
[40] J. Hong, W. Chu, P.A. Chernavskii, A.Y. Khodakov, Journal of Catalysis 273 (2010) 9–17.
[41] Z. Lendzion-Bielun, R. Pelka, W. Arabczyk, Catalysis Letters 129 (2009) 119–123.
[42] D. Varisli, T. Dogu, G. Dogu, Chemical Engineering Science 65 (2010) 153–159.
[43] M. Karthik, A.K. Tripathi, N.M. Gupta, A. Vinu, M. Hartmann, M. Palanichamy, V. Murugesan, Applied Catalysis A 268 (2004) 139–149.
[44] J.S. Beck, J.C. Vartuli, W.J. Roth, M.E. Leonowicz, C.T. Kresge, K.D. Schmitt, C.T.W. Chu, D.H. Olson, E.W. Sheppard, S.B. McCullen, J.B. Higgins, J.L. Schlenker, Journal of the American Chemical Society 114 (1992) 10834–10843.
[45] D. Varisli, T. Dogu, G. Dogu, Industrial and Engineering Chemistry Research 47 (2008) 4071–4076.
[46] G.A. Santos, C.M.B. Santos, S.W. da Silva, E.A. Urquieta-Gonzalez, P.P.C. Confessori Sartoratto, Colloids and Surfaces A 395 (2012) 217–224.
[47] J.M. Jablonski, M. Wolcyrz, L. Krajczyk, Journal of Catalysis 173 (1998) 530–534.
[48] M. Thommes, R. Köhn, M. Fröba, Studies in Surface Science and Catalysis 142 (2002) 1695–1702.
[49] J. Rouquerol, D. Avnir, C.W. Fairbridge, D.H. Everett, J.H. Haynes, N. Pernicone, J.D.F. Ramsay, K.S.W. Sing, K.K. Unger, Pure and Applied Chemistry 66 (1994) 1739–1758.
[50] K.S.W. Sing, D.H. Everett, R.A.W. Haul, L. Moscou, R.A. Pierotti, J. Rouquerol, T. Siemieniewska, Pure and Applied Chemistry 57 (1985) 603–619.
[51] F. Rouquerol, J. Rouquerol, K. Sing, Adsorption by Powders and Porous Solids, Academic Press, San Diego, 1999.
[52] O. Aktas, S. Yasyerli, G. Dogu, T. Dogu, Industrial & Engineering Chemistry Research 49 (2010) 6790–6802.
[53] O. Aktas, S. Yasyerli, G. Dogu, T. Dogu, Materials Chemistry and Physics 131 (2011) 151–159.
[54] T.H. Liou, Chemical Engineering Journal 171 (2011) 1458–1468.